



International Symposium on Room Acoustics
Satellite Symposium of the 19th International Congress on Acoustics
Seville, 10-12 September 2007

ACOUSTICS IN COUPLED ROOMS: MODELLING AND DATA ANALYSIS

PACS: 43.55.Cs

Xiang, Ning¹ and Summers, Jason E.²

¹Graduate Program in Architectural Acoustics, Rensselaer Polytechnic Institute, 110 8th Street, Troy, New York, USA; xiangn@rpi.edu

² Naval Research Laboratory, Washington, D.C. 20375-5350, USA; jason.summers@nrl.navy.mil

ABSTRACT

Acoustical designers are increasingly incorporating coupled rooms in performing-arts spaces. Such designs include reverberant secondary rooms coupled to main audience chambers in concert halls and adaptation of opera houses and theatres for concert-hall use via adjustable orchestra shells that couple audience chambers to stage houses. These applications have prompted research on sound fields in coupled-room systems. Having developed an understanding of the possibilities and limitations of statistical-acoustics (SA) predictions, the validity of geometrical-acoustics (GA) modelling tools has been re-examined. Corrections and improvements are being incorporated into available GA algorithms. Numerical techniques using radiosity and diffusion theory have also emerged to cope with challenges in prediction of acoustics in coupled-room systems. For validation, physical scale-modelling techniques have become particularly relevant research tools. Despite all of these rapid developments, scientifically grounded analysis methods are still needed for objective and subjective evaluations of sound fields in coupled-room systems, whether in terms of numerical modelling, physical scale modelling, or real-hall measurements. After a brief review of modelling techniques, results are presented of Bayesian decay analysis in characterization of sound-energy decays obtained from numerical modelling and experimental measurements.

INTRODUCTION

A number of recently built performing-arts venues contain one or more reverberant auxiliary rooms that are connected to the primary room (audience chamber) in such a way that there is an exchange of acoustic energy. Such configurations constitute systems of coupled rooms. Most representative are two kinds of venues: concert halls, such as *Kultur und Kongresszentrum* Concert Hall (Lucerne, Switzerland) and Myerson-McDermott Hall (Dallas, Texas, USA) in which a reverberant room is coupled to the audience chamber through adjustable openings distributed over the wall surface of the audience chamber; and multipurpose halls, such as Bass Performance Hall (Fort Worth, Texas, USA) and Hall C, Tokyo International Forum (Tokyo, Japan) in which an on-stage orchestra shell divides the stage-house to form a reverberant upper stage-house volume coupled to the orchestra platform and audience chamber through adjustable openings in the orchestra shell.

In addition to enabling variable acoustics, one motivation behind use of coupled rooms is creation of a particular kind of nonexponential sound-energy decay [1, 2]. While exchange of energy between coupled rooms affects other aspects of the sound fields in the coupled subrooms, energy decay has received the greatest attention from practicing acousticians and in psychoacoustic studies. The reasons for this are both historical: when coupled rooms were first modelled, only energy decay could be measured; and empirical: when decays consist of a rapid initial portion followed by a slower late portion, they are believed, but have not been proven, to simultaneously realize the desirable yet competing perceptual attributes of clarity and reverberance.

Effective use of coupled rooms in acoustical design requires predictive models validated by comparison with controlled physical experiments (using scale models) and analysis tools capable of accurately characterizing model outputs and real measurements. In the context of the current focus on decay curves and decay-curve shape, this means frequency-dependent energy-time predictive models and analysis tools able to estimate decay parameters for linear combinations of decaying exponential functions in noise.

NUMERICAL MODELLING

Methods for numerically or computationally modeling the behavior of acoustic energy in rooms are broadly categorized according to whether they are based on a wave or geometrical (particle) model of sound fields. Wave acoustics (WA), the more rigorous of these two approaches, better represents the full phenomenology of acoustic fields including scattering and diffraction. However, it only yields analytical solutions for a few simple cases and is problematic to apply computationally at high frequencies. By contrast, geometrical acoustics (GA), in which sound fields are modeled by ensembles of noninteracting classical phonons, is an inherently high-frequency approach, which though it does not necessarily allow for a greater number of enclosure geometries to be solved analytically, is well suited to various computational implementations. Geometrical acoustics also provides a rigorous base from which to develop statistical models of sound fields. Such models allow for more rapid computation and yield simple, asymptotically correct analytic expressions under certain limiting conditions.

GEOMETRICAL ACOUSTICS (GA)

The classical phonon picture of GA is the basis for the most commonly used modeling techniques in room acoustics. Within this framework, the time-dependent energy (phonon) density $w(\mathbf{r}, t)$ at any point in an enclosure having ideal diffuse reflection (Lambert's law) on the boundaries is given by the integral equation [3]

$$w(\mathbf{r}_r, t) = \frac{W(t - R_{sr}/c)}{4\pi c R_{sr}^2} e^{-mR_{sr}} + \frac{1}{\pi c} \int_S \frac{B(\mathbf{r}, t - R_r/c) [1 - \alpha(\mathbf{r})] \cos \theta_r}{R_r^2} e^{-mR_r} dS, \quad (1)$$

where \mathbf{r}_r is the position of the receiver, $W(t)$ is the time-dependent power of the omni-directional source, R_{sr} is the distance between the source and the receiver, c is the speed of sound, m is the energy-dissipation coefficient of air, \mathbf{r} is the position of an infinitesimal surface element dS , $\alpha(\mathbf{r})$ is the angle-independent absorption coefficient at the surface element, and θ_r is the angle between the normal to the surface element dS and the line joining dS and the receiver position. The integration in the second term on the right-hand side in Eq. (1) is carried out over the entire room surface S . The expression can be modified to account for a general reflection law [4, 5], but yields analytic solutions only in the case of spherical enclosures [4] and infinite parallel plates [6].

Computational GA approaches comprise direct or indirect methods of solving this integral. Acoustical radiosity (AR) attempts to solve some form of Eq. (1) through a direct computational approach of discretization [7]. Typically, it begins with diffuse-reflection form given above. More-conventional methods of computational GA, such as ray tracing, are (for Lambert diffuse reflection on the boundaries) formally equivalent Monte Carlo methods of solving the integral [8].

Making a set of statistical assumptions [9] regarding the aggregate behavior of the phonons yields conventional (Sabine) statistical-acoustics (SA) analytic expressions for the spatially homogenous energy density as a function of time. These assumptions are based on the concept of the diffuse field and are asymptotically correct for ergodic, mixing enclosures in the small-absorption limit. Various semi-empirical corrections to these expressions are possible [see, e.g., 10]. However, expanding a form of the integral equation in a Taylor series in powers of absorption yields the Sabine expression as the zeroth-order term; higher-order terms of the expansion indicate that true first-order corrections must include additional information about particle distributions and enclosure geometry [11]. Alternatively, making only the less-restrictive statistical assumption of ergodicity allows the local phonon density to be equated with the single-particle distribution function [12]. To first order in particle velocity, this yields a diffusion equation describing spatially dependent energy (phonon) density as a function of time [13, 14]. Similar to the discussion above, the conventional (Sabine) SA expression can be related to the diffusion equation by noting that it is the zeroth-order approximation in particle velocity [14]. However, diffusion equations generally must be solved numerically, in contrast with the SA expression.

Statistical-acoustics (SA) models

Single-room SA models such as those of Sabine or Eyring cannot be used generally for coupled rooms [10]. In the general model of coupled rooms described here, the decay from steady state of energy density w in each of the N rooms are expressed in terms of the solutions of a system of N coupled functional differential equations

$$\frac{dw_i(t)}{dt} = -\eta_i \left(2\zeta_i + c \sum_{\substack{j=1 \\ j \neq i}}^N \frac{\bar{\tau}_{ij} S_{ij}}{4V_i} \right) w_i(t) + c \sum_{\substack{j=1 \\ j \neq i}}^N \eta_j \frac{\bar{\tau}_{ij} S_{ij}}{4V_i} \int_{-\Delta_{ij}}^0 w_j(t+s) f_{ij}(s) ds, \quad i = 1 \dots N, \quad (2)$$

where η is a factor determined by the decay model used, which reduces to one for the Sabine decay model (see Ref. [10]), ζ_i is the uncoupled decay constant of the i th room of volume V_i , S_{ij} is the total coupling area between the i th and j th subrooms which has random-incidence transmission coefficient $\bar{\tau}_{ij}$, f_{ij} is the probability density function describing the distribution of propagation delays for this subroom pair, and Δ_{ij} is the maximum delay for this subroom pair.

In general, Eq. (2) must be solved numerically even if f_{ij} is a delta function (yielding a system of delay differential equations). However, in the limiting case that f_{ij} is a delta function centered at zero for all i and j , the resulting system of ordinary differential equations is solved conventionally by expressing it in matrix form and noting that the steady-state conditions are given by the solution of the system of coupled energy-balance equations

$$\frac{W_m}{V_m} = -\sum_{n=1}^N \psi_{mn} w_{mn}(0), \quad m = 1 \dots N, \quad (3)$$

where W_m is the time-averaged power of the source located in the m th room. The solutions take the form of a linear combination of decaying exponential functions, the number of terms in the linear combinations being equal to the number of subrooms.

The breakdown of this model and additional corrections are discussed in Ref. [10]. These corrections primarily address nondiffuse transfer of energy between subrooms and line-of-sight energy transfer between nonadjacent subrooms. Nonetheless, the model is generally able to well predict decay behavior in cases of sufficiently weak coupling and subrooms that satisfy the requirements of SA decay models, as shown in Fig. 1.

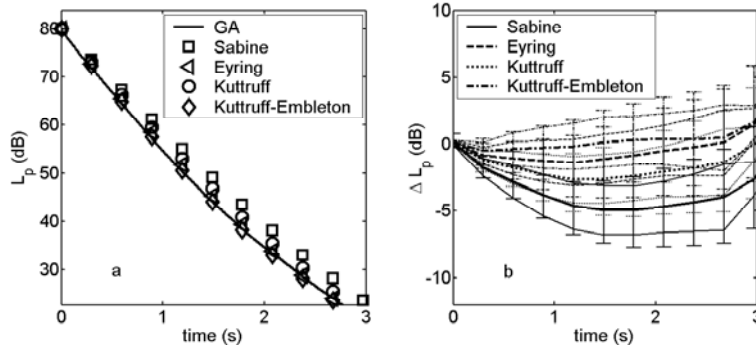


Figure 1.- For a two-room coupled system with high, nonuniform absorption in the source room, ensemble averages of computational GA-model predictions (with diffuse surface reflection) for all sources and receivers the source room (solid line) are compared with SA-model predictions of Eq. (2) (for delta function delays centered at zero) using Sabine (squares), Eyring (triangles), Kuttruff (circles), and Kuttruff-Embleton (diamonds) decay models for $S_{12} = 25 \text{ m}^2$ (a). Differences between GA and SA predictions ($10 \log_{10} \text{GA} - 10 \log_{10} \text{SA}$) [using Sabine (solid line), Eyring (dashed line), Kuttruff (dotted line), and Kuttruff-Embleton (dot-dash line) decay models] are plotted for $S_{12} = 25 \text{ m}^2$ (b). The regions of confidence are plotted as error bars for SA predictions and as fainter lines lying on either side of the primary lines for GA predictions. Confidence limit predictions assume input parameters are known to $\pm 10\%$ at the same level of confidence.

Diffusion-equation (DE) models

Allowing the assumption of ergodicity, energy density $w(\mathbf{r}, t)$ as a function of position \mathbf{r} and time t is given to first order by the diffusion equation

$$\frac{\partial w(\mathbf{r}, t)}{\partial t} - D \nabla^2 w(\mathbf{r}, t) + c m w(\mathbf{r}, t) = F(\mathbf{r}, t) \quad \in V, \quad (4)$$

subject to the boundary condition on the interior surface S ,

$$D \frac{\partial w(\mathbf{r}, t)}{\partial n} + c A w(\mathbf{r}, t) = 0, \quad (5)$$

where Eq. (4) is the interior equation for the subroom denoted by domain V having a source term $F(\mathbf{r}, t)$, which is zero for any subroom where no source is present. The diffusion coefficient is given by $D = \lambda c / 3$, where λ is the mean free path. The term $c m w(\mathbf{r}, t)$ accounts for air dissipation in the room(s), and can be extended for accounting for absorption due to scattering objects inside the room(s) [16]. The absorption term, A can take the following forms

$$A_S = \frac{\alpha}{4}, \quad (6a)$$

$$A_E = \frac{-\ln(1 - \alpha)}{4}, \quad (6b)$$

or

$$A_M = \frac{\alpha}{2(2 - \alpha)}. \quad (6c)$$

The term A_S has been used in room-acoustics predictions since Ollendorf 1969 [13]. More recently, Jing and Xiang [17] and Billon et. al. [18] independently proposed the absorption term A_E in Eq. (6b) for modeling cases where surfaces of the room under test have high overall absorption. Diffusion equations using the absorption terms A_S or A_E in Eqs. (6a-b) are designated as the diffusion-Sabine model or diffusion-Eyring model, respectively [18]. The term A_M in Eq. (6c) has been derived most recently by Jing and Xiang [19], who have demonstrated that the diffusion equation with this modified absorption term in the boundary condition is theoretically grounded and can model both low and high absorption surfaces.

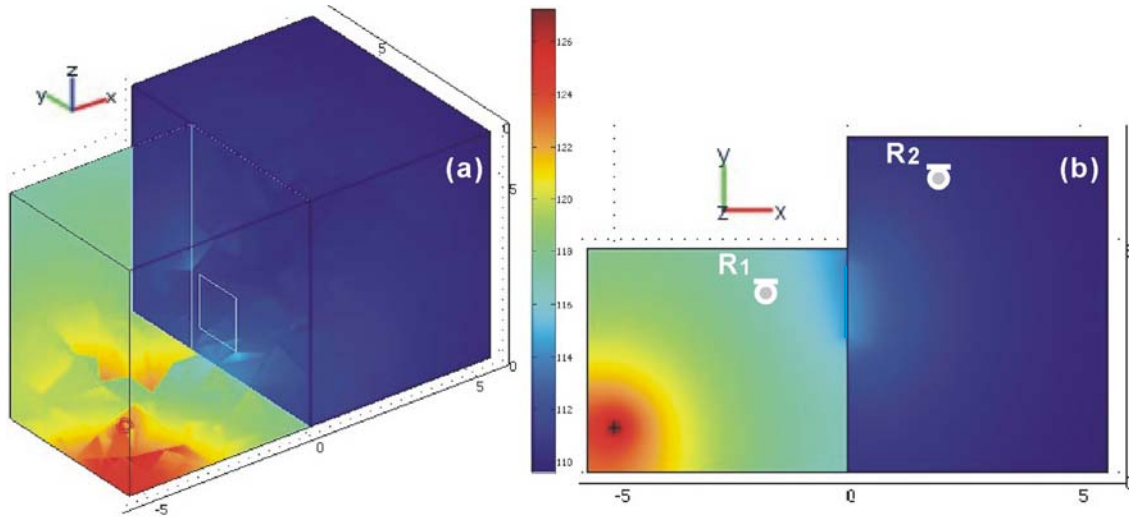


Figure 2. Mapping of sound pressure level distributions using the modified diffusion equations in rooms of a coupled-volume system. The dimensions correspond to the original sizes of the experimental models shown in Fig. 3. (a) Partially transparent 3D view into the coupled rooms showing the meshing and aperture size and location. (b) 2D mapping showing the source location and sound fields across two coupled rooms. A point source location is marked by '+'.

The diffusion equation method has been applied to modelling a wide variety of enclosure types, such as long rooms, flat rooms, fitted rooms, and coupled rooms [15, 17, 20, 21]. In modelling coupled rooms, the domain V comprises an arbitrary number of subdomains, which are the subrooms of the coupled-room system. Diffusion coefficients for each subroom are assigned based on the mean free path of each subroom under the assumption that coupling these subrooms does not significantly change their free path distributions. Coupling configurations with weak coupling (small coupling apertures) approximately meet this assumption (see the discussion in Ref. [10]).

Figure 2 illustrates the predicted sound pressure level (SPL) distributions within a two-room coupled system. Equations (4-5) were solved by a finite-element method using a total of 8000 linear Lagrange-type mesh elements. The stationary SPL distribution is determined after solving for $w(\mathbf{r})$ from Eqs. (4-5) by including the contribution of the direct field

$$L_p(\mathbf{r}) = 10 \log \left\{ \frac{\rho c}{P_{ref}^2} \left[\frac{P_s}{4\pi r^2} + w(\mathbf{r})c \right] \right\}, \quad (7)$$

where ρ is the air density, and r is the source-receiver distance. Figure 3 illustrates two normalized energy decay functions at receiver position R_1 and R_2 , indicated in Fig. 2(b).

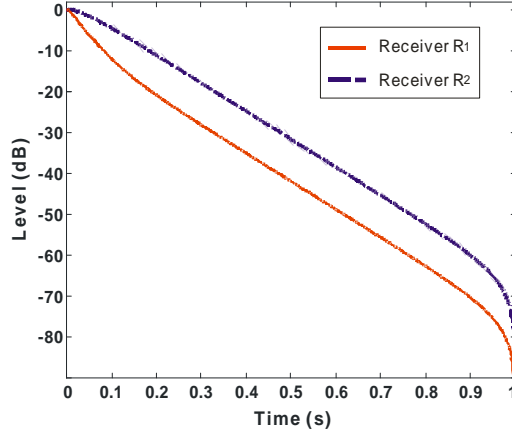


Figure 3. Steady-state sound energy decay functions simulated at receiver position marked by R_1 , R_2 in Fig.2(b).

Computational Geometrical-acoustics (GA) models

Image-source [22] and ray-tracing [23-24] methods, the two traditional methods used for computational modelling of sound fields in rooms according to the laws of GA, display no fundamental limitations unique to coupled-room configurations. Rather, they only require careful implementation allowing for more complex visibility checks and the possible requirement of more rays [25-27] to provide for the more stringent requirements on spatial sampling (Chap. 6 of Ref. [28]). However, image-source and ray-tracing methods have been largely superseded commercially by more modern variations on these algorithms (cone- or beam-tracing) and hybrid approaches [29-31].

With the increasing need of commercial software to simulate coupled rooms, the validity of these modelling tools has been re-examined [32]. In commercial beam-tracing software, beam tracing is most often applied approximately, by tracing only the central axes of the beams—so-called beam-axis tracing. This approach offers the advantage of decreased computing time by covering the 4π sr of solid angle outwardly visible from the source more efficiently than ray tracing (i.e., fewer beam-axis are needed than rays due to the increased detection probability of a beam face relative to a ray.) However, it can result in incorrect detections of energy arrivals at receivers in the late part of the decay, which must be addressed by a tail-correction procedure. Likewise, hybrid methods often require some form of tail correction or must make assumptions regarding the nature of the late decay.

Conventionally, correction algorithms assume that the reflection density $n(t)$ is quadratic in time following the expression

$$n(t) = \frac{4\pi c^3 t^2}{V} \quad (8)$$

or, more generally, assume that $n(t) \propto t^2$ and determine the constant of proportionality by curve fitting. However, these assumptions do not hold in coupled rooms, as the reflection density associated with each subroom may differ, such that the function describing $n(t)$ can vary with both time and position.

In recent work [32], the beam-axis-tracing algorithm RTC used by the commercial software CATT-Acoustic was modified to eliminate both of these sources of error when modelling coupled rooms. The new algorithm

behaves as RTC until any one of the expanding detector spheres contacts one of the surface boundaries. From that point on, rather than applying tail-correction, the radius of each detection sphere is held fixed and the detection procedure at each receiver is altered to that of ray-tracing (i.e., the propagation law of r^{-2} is addressed by changes in detection probability due to ray divergence, rather than explicit reduction of the energy associated with each ray). In addition, effects of diffraction are often significant in coupled rooms [27], recent effort in improving / including diffraction phenomena in GA modelling [33] is expected to contribute to effective modelling of coupled rooms.

While Kang [34], Nosal et al. [7], and Zhang [35] have detailed use of the AR method, only recently work has been directed toward using it in coupled rooms [36]. As with other computational GA methods, implementation may require some specific adaptations for coupled rooms.

WAVE ACOUSTICS

Various methods are available for the analytic and computational solution of the time-harmonic (steady-state) and time dependent wave equations in coupled rooms. Prior work in this area up through 2003 has been surveyed in detail in Ref. [28]. More recently, additional work on time-harmonic fields in coupled rooms using (and improving upon) well-established finite-element methods has been published [37-38]. Additionally, Meissner [39] has described a numerical solution method that can predict steady-state and time-dependent fields in systems of coupled rooms given that the light-damping assumption is satisfied. Despite development of these techniques, application of wave-based computational methods to auditoria is fundamentally limited in the audible range of frequencies by high modal density and a chaotic dependence of field parameters on small perturbations of the boundary.

PHYSICAL MODELLING

The classical alternative to intractable wave-acoustics problems has been physical modelling. Rayleigh was the first to observe that wave phenomena, neglecting fluid properties of the medium, are determined by the size of the wavelength relative to the size of the scattering object and therefore are independent of absolute scale. This observation allows for scale models to be used to study acoustical phenomena—including scattering and diffraction—provided that the wavelength of the sound is also appropriately scaled. In room acoustics, the use of such models originated with Spandoeck [38]. In order to uniquely describe the sound field of an enclosure, the boundary conditions on the surface of the enclosure must be described by complex impedance, which is generally a function of both frequency and angle of incidence. Ideally, a scale model should employ surfaces that reproduce the impedance of the actual surfaces at the scaled frequency. In practice, this is very difficult and it is typical to instead specify surfaces for scale model applications by absorption coefficient. Even so, the viscothermal apparent absorption will be different in the model than in the actual space and thus must be corrected, such as by replacing air by nitrogen [41].

Validation

However, because scale models provide a controlled environment in which the geometry and material properties can be known with high precision, they are the ideal method for validating mathematical and computational models of sound fields in coupled rooms. Here, the goal is to know material properties to a high degree of accuracy, rather than match them to the properties of particular full-scale materials. Recent applications of acoustical scale-modelling for validation can be found, amongst others in Refs. [41-43], and, for coupled rooms, in Ref. [32]. With advanced acoustical measurement techniques [45], scale-model measurements [41] can be accomplished with satisfactory signal-to-noise ratio using maximum-length sequences or sweep signals [46].

Auralization

With the increasing need for psychoacoustic evaluations of coupled-room soundfields [47], binaural scale modelling [41] offers another significant use. Wave phenomena, such as diffraction from coupling apertures and spatial variation due to modal distributions, may have significant subjective effects but are difficult to model computationally. However, binaural scale modelling technique (so-called scale-modelling auralization) [41] has been developed and can provide psychoacoustic studies with well-characterized binaural impulse responses having high physical accuracy.

BAYESIAN DECAY ANALYSIS

Despite multiple developments in physical and numerical modelling techniques, little attention has been given to developing effective and efficient tools for analyzing the results of modelling and measurement.

This holds true even in the case of methods for quantifying energy decay characteristics, one of the most salient and widely discussed aspects of acoustical behaviour in coupled rooms.

Schroeder decay model

Most numerical modelling tools are able to deliver energy impulse responses. Likewise, modern techniques [45-46] can provide acousticians with experimentally measured room impulse responses (RIR) of high quality. Using energy RIR obtained from either numerical modelling or experimental measurements, Schroeder backward integration [48] yields the energy-decay response from steady state, energy-decay functions $\mathbf{D} = [d_1, d_2, \dots, d_K]^{Tr}$, where $(\cdot)^{Tr}$ stands for matrix transpose, and K is the total number of data points in \mathbf{D} . In modelling Schroeder decay functions, a parametric model has been proposed [49-50]:

$$\mathbf{D} = \mathbf{G}_m \mathbf{A}_m + \mathbf{e}, \quad (10)$$

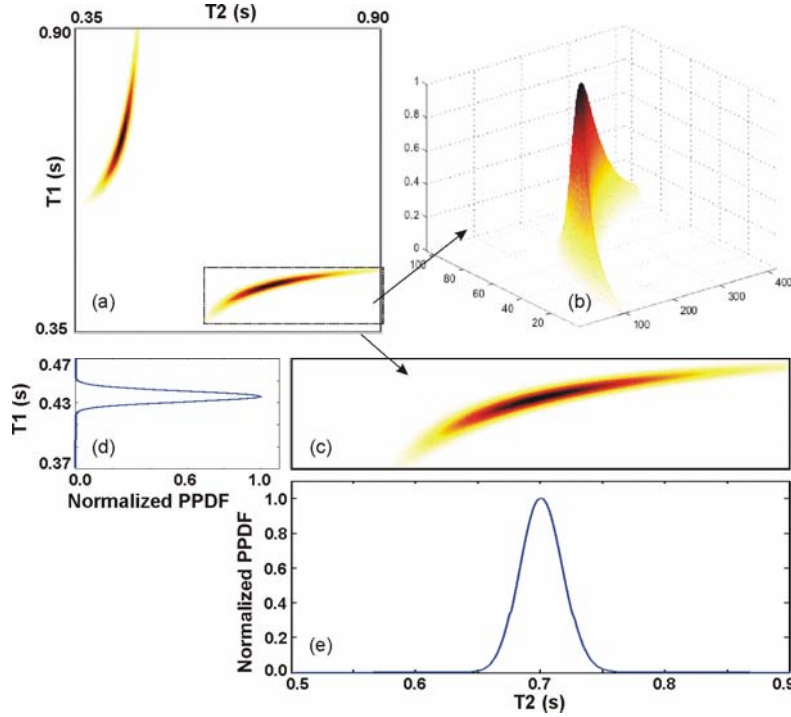


Figure 5. Posterior probability density function (PPDF) of decay times evaluated from a Schroeder decay function measured in scale-model coupled spaces. (a) PPDF in 2-D representation over $T_{1,2}$ within $\{0.35, 0.9\}$ s. (b) PPDF in 3-D representation over a subspace evaluated with a grid of 108×420 . (c) A-zoomed PPDF over T_1 within $\{0.37, 0.47\}$ s, T_2 within $\{0.5, 0.9\}$ s. (d), (e) projection of the line across the peak PPDF onto individual decay time axis.

which approximates the data \mathbf{D} with an error vector \mathbf{e} ; where \mathbf{A}_m is a column vector of $(m+1)$ amplitude coefficients, termed *linear parameter vector*; \mathbf{G}_m is a $K \times (m+1)$ matrix; and m is the number of decay rates or *model order*. The j th column of \mathbf{G}_m is given by its matrix element

$$g_{kj} = \begin{cases} t_k - t_K & \text{for } j=0 \\ \exp(-13.8 \cdot t_k / T_j) - \exp(-13.8 \cdot t_K / T_j) & \text{for } j=1,2,\dots,m \end{cases}, \quad (11)$$

where T_j is j th decay time to be determined for $1 \leq j \leq m$, $T_0 = \infty$. The quantity t_K represents the upper limit of Schroeder's integration, $0 \leq k < K-1$. Specifically, for $m=2$ with a large enough t_K , the decay Schroeder model becomes

$$\mathbf{G}_2 \mathbf{A}_2 \approx A_0(t_k - t_K) + A_1 \exp(-13.8 \cdot t_k / T_1) + A_2 \exp(-13.8 \cdot t_k / T_2) \quad (12)$$

Bayesian decay-parameter estimation

Given an appropriate decay model, Bayesian theory formulates the posterior probability density function (PPDF) of model parameters through the prior probability density and likelihood function via Bayes' theorem:

$$p(\mathbf{A}, \mathbf{T} | \mathbf{D}, I) = \frac{p(\mathbf{A}, \mathbf{T} | I) p(\mathbf{D} | \mathbf{A}, \mathbf{T}, I)}{p(\mathbf{D} | I)}, \quad (13)$$

where $p(\mathbf{D} | I)$ acts in the context of parameter estimation as a normalization constant; \mathbf{T} is a vector matrix of m decay times; and $p(\mathbf{A}, \mathbf{T} | I)$ is the prior distribution function of \mathbf{A} and \mathbf{T} . Bayes' theorem in Eq. 13 represents how prior knowledge $p(\mathbf{A}, \mathbf{T} | I)$ is updated in the light of data through the likelihood function $p(\mathbf{D} | \mathbf{A}, \mathbf{T}, I)$. Background information I here includes that the Schroeder decay model in Eqs. 10-12 describes the data \mathbf{D} reasonably well so that all errors in \mathbf{e} are bounded by a finite value. Given finite errors and a reasonable model as the available information, application of the principle of maximum entropy [51] assigns a Gaussian distribution to the likelihood function $p(\mathbf{D} | \mathbf{A}, \mathbf{T}, I)$ and yields independent errors e_i , so that

$$p(\mathbf{D} | \mathbf{A}, \mathbf{T}, \sigma, I) = (\sqrt{2\pi}\sigma)^{-K} \exp\left(-\frac{\mathbf{e}^{Tr} \mathbf{e}}{2\sigma^2}\right), \quad (14)$$

with a finite, but unspecified error variance σ^2 . Probability theory provides rules of relating and manipulating the quantities, leading to an analytically tractable PDF in form of the student-T distribution:

$$p(\mathbf{T} | \mathbf{D}, I) \propto (\mathbf{D}^{Tr} \mathbf{D} - \mathbf{q}^{Tr} \mathbf{q})^{-(m-K)/2}, \quad (15)$$

with $\mathbf{q} = \mathbf{Q}^{Tr} \mathbf{D}$ and $\mathbf{Q} = \mathbf{G} \mathbf{E} \mathbf{A}^{-1}$ [52]. Figure 5 illustrates a PDF (Eq. 15) over parameter space $\{T_1, T_2\}$ using a Schroeder decay model of order two, evaluated from a room impulse response measured in a scale-model system of two coupled rooms. Localizing maximum values of the PDFs, so-called maximum a posteriori (MAP) approaches [52] or probabilistic approaches based on Markov chain Monte Carlo (MCMC) methods [53-54] have been used in room-acoustic energy decay analysis, where the uncertainties of inferred decay parameters can also be quantitatively estimated [54] through a covariance matrix $[C_{ij}]$ with its expected matrix element:

$$\langle C_{ij} \rangle \approx \frac{\sum_{r=1}^R (T_{ir} - \langle T_i \rangle)(T_{jr} - \langle T_j \rangle) u(\mathbf{T}_r)}{\sum_{r=1}^R u(\mathbf{T}_r)}, \quad (16)$$

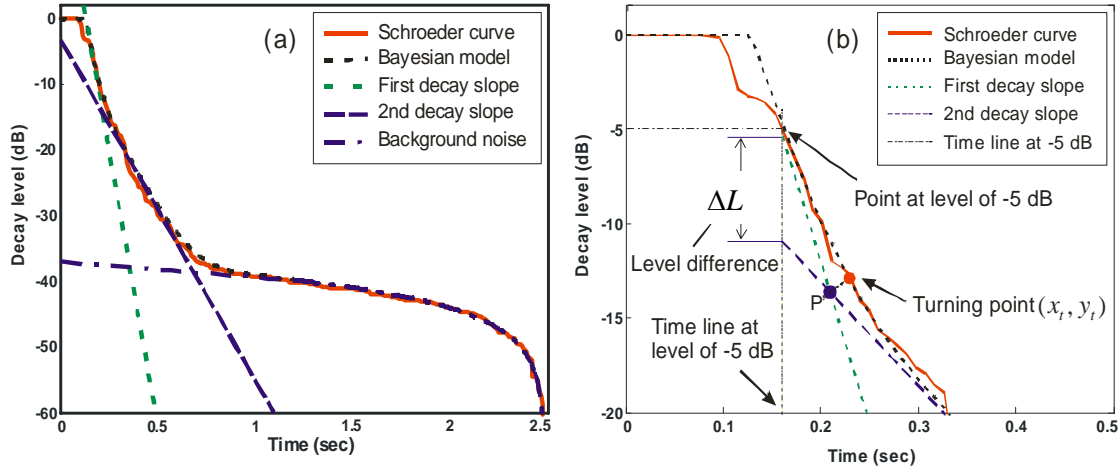


Figure 6. Steady-state sound energy decay functions simulated at receiver position marked by R_1, R_2 in Fig.4(b).

where

$$u(\mathbf{T}_r) = \frac{p(\mathbf{T}_r | \mathbf{D}, I)}{g(\mathbf{T}_r)}, \quad (17)$$

$g(\mathbf{T}_r)$ is the random process used to draw R samples from $p(\mathbf{T} | \mathbf{D}, I)$ in Eq. 15, and $\langle T_i \rangle$ is the expected mean value of decay time T_i . In this way, the standard deviations of individual estimated parameters, and dependences between parameters can also be estimated from the covariance matrix $[C_{ij}]$ via Eqs.15-17 [54].

Relevant decay parameters

Figure 6 (a) illustrates a double-slope decay function, measured in a scale-model system of two coupled rooms, in comparison with its Schroeder decay model. Bayesian analysis, using the model in Eq. (12), yields

three model terms, as plotted in the Fig. 6(a). Figure 6 (b) gives a magnified view of the first 20 dB. Because the early portion of the energy decay represents only a small number of short-delay paths, it cannot be modelled by Eqs. 10-12. Instead, the first 5 dB should be excluded, as recommended by ISO 3382 [55]. The data analysis illustrated in Fig. 6 (as well as all other data analysis throughout this work) is undertaken from -5dB to the end of the data record.

Bayesian analysis provides the amplitude parameters, decay times, associated uncertainties, and mutual dependence. In Eq. 12, A_0 is associated with the background noise in the room impulse response, actually a nuisance parameter, being a necessary part of the model, but of insignificant relevance for the energy decay analysis. In addition to the individual decay times, architectural acousticians are interested in the relative amplitude A_2 with respect to A_1 for double-slope cases, rather than their individual values. The decay-level difference ΔL in decibels, first used by Xiang and Goggans [51], is defined as

$$\Delta L = 20 \lg(A_1 / A_2) \Big|_{at=-5dB} \quad (\text{dB}) \quad (18)$$

Figure 6(b) illustrates this definition and further indicates the reason that the reverberation analysis is undertaken using the data segment from -5 dB point. The decay-level difference quantifies how low the second decaying process characterized by T_2 is relative to the first one of T_1 .

Table I lists Bayesian decay analysis from a room impulse response experimentally measured in the Student Union at the University of Mississippi over the octave frequency bands from 125 Hz to 2 kHz. Table I also lists the standard deviations (Std) of T_i .

Table I.- Calculated decay parameters across the octave bands from a room impulse response measured in the Student Union at University of Mississippi.

Band (Hz)	T_1 (s)	Std ₁ (s)	T_2 (s)	Std ₂ (s)	Decay Time Ratio	Level difference ΔL (dB)	Turning point	
							T_t (s)	L_t (dB)
125	0.71	6.87E-3	2.82	4.67E-2	3.93	2.60	0.281	-10.43
250	0.68	2.91E-3	2.38	2.09E-2	3.46	3.54	0.282	-11.42
500	0.99	3.20E-3	2.74	5.43E-2	2.75	7.13	0.383	-16.91
1000	0.88	1.82E-3	2.63	4.22E-2	2.99	9.47	0.412	-19.47
2000	0.92	3.03E-3	--	--	--	--	--	--

In Fig. 6(b) two straight lines corresponding to two decay slopes in logarithmic presentation can be determined

$$y_j = a_j + b_j \cdot t_k, \quad (19)$$

with $a_j = 10 \cdot \lg A_j$, $b_j = -10 \cdot \lg e \cdot (13.8/T_j)$, $j=1, 2$ Bayesian decay-parameter estimation in the case of a double-slope decay yields two straight lines corresponding to the two decay slopes, which, in general, will not cross at a point coincident with the turning point of the data (Schroeder curve) and model decay curve. Rather, the crossing point $P'(x_0, y_0)$ given by:

$$x_0 = (a_2 - a_1)/(b_1 - b_2), \quad y_0 = (a_2 b_1 - a_1 b_2)/(b_1 - b_2), \quad (20)$$

will generally be lower in level. The turning point $P_t(x_t, y_t)$ is defined to be a point on the decay model curve, to which the crossing point (P') has the minimum distance:

$$\sqrt{(x_t - x_0)^2 - (y_t - y_0)^2} \rightarrow \min. \quad (21)$$

Two decay times or decay ratio (T_2/T_1), along with the level difference (ΔL in dB), the co-ordinate of the turning point (x_t, y_t) are relevant decay parameters, eventually used for further studies of acoustics in coupled rooms.

DISCUSSION AND CONCLUSIONS

Comparison of model techniques

Correctly implemented, SA methods can accurately predict spatially averaged energy-decay behaviour in systems of coupled rooms with very minimal computational expense (a few seconds of computation time). Moreover, incorporating semi-empirical geometrical corrections allows modelling of the courser aspects of

location-dependent decay [10]. Diffusion-equation (DE) models provide greater spatial information and less restrictive assumptions. Yet, the computational expense of DE is relatively low because the mesh used for the finite element solution is directly dependent on the order of mean free path, but not on the acoustic wavelength. The computational load using currently available laptop PC for modelling the stationary sound energy distribution throughout the domains in rooms as shown in Fig. 2 is on the order of a minute. For computing energy decays at each receiver position as shown in Fig.3, it takes a few minutes for a time-resolution of 10 ms. Computational geometrical-acoustics (GA) methods provide greater details still, but with increasing computational expense. However, because such models provide information about discrete reflections as a function of time, they are uniquely able to facilitate auralization. Different techniques vary in the distribution of their computational load. The computational expense of the acoustical radiosity (AR) method is relatively high, yet the computation costs are mostly incurred only in the initial rendering of the room(s) under test [7]. Once the rooms have been rendered for a given source, the remaining computational load is low. In contrast, ray- and beam-tracing methods typically have computational costs that scale with the number of source-receiver combinations to be modelled.

Frequency and location dependence

Sound fields in coupled rooms are the result of complex interactions between the sound fields of multiple subrooms. This increased complexity over single-volume rooms results in greater opportunities for location and frequency dependence in the acoustical behaviour [10, 27]. Moreover, modeling techniques that are tractable at high-frequencies (GA) make certain limiting physical assumptions. Thus, techniques for modeling soundfields in rooms are inherently frequency-dependent for both practical and theoretical reasons. Similarly, analysis techniques need to reflect these physical realities by considering variations in both frequency and location. For sound fields in single-volume rooms, high- and low-frequency regions in which geometrical and wave acoustics, respectively, are appropriate are defined by the relation of wavelength to characteristic dimension of the room. This classic two-region paradigm leaves a gap in the mid-frequency region where geometrical acoustics is inaccurate but wave acoustics is untenable. In the case of coupled-room auditoria, this gap is particularly notable because the defining aspect of coupled rooms, the exchange of energy between subrooms, takes place through apertures having typical length scales corresponding to wavelengths in this mid-frequency region. Summers has proposed a three-region heuristic to address this [27, 56-57], in which conventional high- and low-frequency models are supplemented by mid-frequency models that explicitly address the effects of diffraction at coupling apertures [56, 10]. Most recently, Pu et. al. [58] has conducted experimental investigations on spatial distributions of sound energy flows and energy decays in scale-down coupled rooms.

The role of scale modelling

Development of new computational modelling methods always requires verification of the algorithms and validation of the underlying physics. As new techniques for modelling coupled rooms continue to develop, scale models provide the most effective and controlled means of providing the data necessary for validation. Likewise, they provide a controlled means of generating highly accurate RIR for psychoacoustical studies.

Noise-tail compensation

Some existing data-analysis approaches attempt to accurately estimate the nuisance parameter in order to compensate for the noise tail of the Schroeder decay function [the first term in Eq. (12)]. However, given the analysis tools discussed in this paper, such noise-compensation techniques, with their heavy reliance on accurate estimation of the nuisance parameter, are not recommended, especially for nonexponential decays. Noise compensation does not solve the problems of resolving relevant decay parameters. Compensation is often based on under or over estimation, which can destroy the decay characteristics in the measured data leading to biased estimations of the relevant decay parameters.

Linear fitting of predefined decay portions

Successful application of Bayesian analysis to the validated Schroeder decay model [Eq. (12)] of sound-energy decay unambiguously demonstrates that other methods for evaluating nonexponential decays, including those which compare linear fits of different portions of logarithmic decay functions (e.g., T15 vs. T20, or T10 vs. T of an arbitrarily chosen portion between -30 and -40 dB) are scientifically questionable. Quantifiers cannot generally provide a unique description for a nonexponential decay consisting of a linear combination of decaying exponential functions. Thus, despite their ease of implementation, such techniques should no longer be practiced.

Acknowledgement

N.X. is grateful to Damian Doria at Artec Consultants Inc and Robert Berens at Acentech Inc for their support. Thanks are also due to Prof. J. Kang for his constructive suggestions. J.E.S. is currently supported by ONR with past support for this work from the Bass Foundation, RPG Diffusor Systems, and Rensselaer Polytechnic Institute.

References

1. J. C. Jaffe, Selective reflection and acoustic coupling in concert hall design, *Proc. Music & Concert Hall Acoustics, MCHA 1995*, ed. Y. Ando and D. Nason, Academic Press, New York (1995) 85-94.
2. R. Johnson, E. Kahle, and R. Essert, Variable coupled volume for music performance, *Proc. Music & Concert Hall Acoustics, MCHA 1995*, ed. Y. Ando and D. Nason, Academic Press, New York (1995) 372-385.
3. H. Kuttruff, Simulierte Nachhallkurven in rechteckräumen mit diffusem schallfeld, (Simulated decay curves in rectangular rooms with diffuse sound fields.) *ACUSTICA 25* (1971) 333-342. [See H. Kuttruff, *Room acoustics*, 4th ed. Spon Press (2000) for a presentation in English.]
4. W. B. Joyce, The exact effect of surface roughness on the reverberation time of a uniformly absorbing spherical enclosure, *J. Acoust. Soc. Am.* **64** (1978) 1429-1436.
5. A. Le Bot, A functional equation for the specular reflection of rays, *J. Acoust. Soc. Am.* **112** (2002) 1276-1287.
6. H. Kuttruff, Stationary propagation of sound energy in flat enclosures with partially diffuse surface reflection, *ACUSTICA 86* (2000) 1028-1033. (See also references therein.)
7. E.-M. Nosal, M. Hodgson, and I. Ashdown, Improved algorithms and methods for room sound-field prediction by acoustical radiosity in arbitrary polyhedral rooms, *J. Acoust. Soc. Am.* **116** (2004) 970-980.
8. A. Le Bot and A. Bocquillet, Comparison of an integral equation on energy and the ray-tracing technique in room acoustics, *J. Acoust. Soc. Am.* **108** (2005) 1732-1740.
9. W. B. Joyce, Sabine's reverberation time and ergodic auditoriums, *J. Acoust. Soc. Am.* **58** (1975) 643-655.
10. J. E. Summers, R. R. Torres, Y. Shimizu, Statistical-acoustics models of energy decay in systems of coupled rooms and their relation to geometrical acoustics, *J. Acoust. Soc. Am.* **116** (2004) 958-969.
11. W. B. Joyce, Power series for the reverberation time, *J. Acoust. Soc. Am.* **67** (1980) 564-571.
12. T. Le Pollès, J. Picaut, S. Colle, M. Bérengier, and C. Bardos, Sound-field modelling in architectural acoustics by a transport theory: Application to street canyons, *Physical Review E* **72** (2005) 046609.
13. F. Ollendorff, Statistical room-acoustics as a problem of diffusion: a proposal, *Acustica 21* (1969) 236-245.
14. J. Picaut, L. Simon, and J. D. Ploack, A mathematical model of diffuse sound field based on a diffusion equation, *Acustica united with Acta Acustica 83* (1997) 614-621.
15. V. Valeau, J. Picaut, and M. Hodgson, On the use of a diffusion equation for room-acoustic prediction, *J. Acoust. Soc. Am.*, **119** (2006) 1504-1513.
16. V. Valeau, M. Hodgson, and J. Picaut, A diffusion-based analogy for the prediction of sound fields in fitted rooms, *Acustica united with Acta Acustica 93* (2007) 94-105.
17. Y. Jing and N. Xiang, A modified diffusion equation for room-acoustic prediction (L), *J. Acoust. Soc. Am.*, **121** (2007) 3284-3287.
18. A. Billon, J. Picaut, and A. Sakout, Prediction of the reverberation time in high absorption room using a modified-diffusion model, *Applied Acoustics* (2007, in print).
19. Y. Jing and N. Xiang, On boundary conditions for the diffusion equation in room-acoustic prediction, *J. Acoust. Soc. Am.*, (2007, submitted)
20. V. Valeau, J. Picaut, A. Sakout, and A. Billon, Simulation of the acoustics of coupled rooms by numerical resolution of a diffusion equation, *Proc. ICA 2004, Japan*.
21. A. Billon, V. Valeau, A. Sakout, and J. Picaut, On the use of a diffusion model for acoustically coupled rooms, *J. Acoust. Soc. Am.*, **120**, 2006, pp. 2043-2054.
22. B. M. Gibbs and D. B. Jones, A simple image method for calculating the distribution of sound pressure levels within an enclosure, *ACUSTICA 26* (1972) 24-32.
23. M. R. Schroeder, B. S. Atal, and C. Bird, Digital Computers in room acoustics, *Proc. 4th ICA*.
24. A. Krokstad, S. Strøm, and S. Sørsdal, Calculating the acoustical room response by the use of a ray tracing technique, *Journal of Sound & Vibration 8* (1968) 118-125.
25. U. Ayr. E. Cirillo, and F. Martellotta, Theoretical and experimental analysis for coupled rooms transient behaviour and relevant acoustical parameters, *Proc. 17th ICA, Roma 2001*.
26. L. Nijs, G. Jansens G. Vermeir, and M. van der Voorden, Absorbing surfaces in ray-tracing programs for coupled spaces, *Applied Acoustics 63* (2002) 611-626.
27. J. E. Summers, Comments on "Absorbing surfaces in ray-tracing programs for coupled spaces", *Applied Acoustics 64* (2003) 825-831.
28. J. E. Summers, Reverberant Acoustic Energy in Auditoria that Comprise Systems of Coupled Rooms (Ph.D. Dissert., Rensselaer Polytechnic Institute, Troy, NY 2003) [*J. Acoust. Soc. Am.* **114**, 2526 (A) (2003)]. (E-copies are available from the author.)
29. M. Vorlaender, Simulation of the transient and steady-state sound propagation in rooms using a new combined ray-tracing / image-source algorithm, *J. Acoust. Soc. Am.* **86** (1989) 172-178.
30. G. M. Naylor, ODEON – Another hybrid room acoustical model. *Applied Acoustics 38* (1993) 131-143.
31. B.-I. L. Dalenbäck, "Verification of prediction based on Randomized Tail-Corrected cone-tracing and array modeling," on the CD-ROM: Berlin, March 14-19, Collected Papers, 137th Meeting of the Acoustical Society of America and the 2nd Convention of the European Acoustical Association (ISBN 3-9804458-5-4, available from Deutsche Gesellschaft für Akustik, Fachbereich Physik, Universität Oldenburg, 26111 Oldenburg, Germany), paper 3pAAa1 (1999) [*J. Acoust. Soc. Am.* **105**, 1173 (A) (1999)].
32. J. E. Summers, R. R. Torres, Y. Shimizu, and B.-I. L. Dalenbäck, Adapting a randomized beam-axis-tracing algorithm to modelling of coupled rooms via late-part ray tracing, *J. Acoust. Soc. Am.* **118** (2005) 1491-1502.
33. U. P. Svensson and P. Calamia, Edge-diffraction impulse responses near specular-zone and shadow-zone boundaries, *Acta Acustica united with Acustica*, **92**, (2006) 501-512.
34. J. Kang, Reverberation in Rectangular Long Enclosures with Diffusely Reflecting Boundaries, *Acustica united with Acta Acustica*, **88** (2002), 77-87.
35. H. Zhang, Relaxation of sound fields in rooms of diffusely reflecting boundaries and its application in acoustical radiosity simulation, *J. Acoust. Soc. Am.* **119** (2006) 2189-2200.
36. G. Jiang and X. Zhang, A radiosity model for sound decays in coupled rooms, *Proc. 3rd Inter. Symposium on Temoral Design in Architecture and Environment*, GuangZhou, China, Nov. 2007.
37. G. Bartsch: Effiziente Methoden für die niederfrequente Schallfeldsimulation (Efficient methods for low-frequency sound-field simulation) (Ph.D. Dissertation, RWTH, Aachen, 2003).

38. Y. Zhao and S. Wu: Acoustical normal-mode analysis of two coupled rooms, *Proc. 21st International Conference of the Audio Engineering Society*, St. Petersburg, Russia (2002).
39. M. Meissner: Computational studies of steady-state sound field and reverberant sound decay in a system of two coupled rooms, *Central European Journal of Physics* **5**, No. 3 (2007) 293-312.
40. F. Spandoeck, Akustische Modellversuche, *Annalen der Physik*, **20** (1934) 345-360.
41. N. Xiang & J. Blauert, Binaural Scale Modelling for Auralization and Prediction of Acoustics in Auditoria, *Applied Acoustics* **38** (1993) 267-290.
42. S. Chiles and M. Barron, Sound level distribution and scatter in proportionate spaces, *J. Acoust. Soc. Am.* **116** (2004) 1585-1595.
43. J. Jeon, and M. Barron, Evaluation of stage acoustics in Seoul Arts Center Concert Hall by measuring stage support, *J. Acoust. Soc. Am.* **117** (2005) 232-239.
44. W. Yang and M. Hodgson, Ceiling baffles and reflectors for controlling lecture-room sound for speech intelligibility, *J. Acoust. Soc. Am.* **121** (2007) 3517-3326.
45. N. Xiang, and M. R. Schroeder, Reciprocal maximum-length sequence pairs for acoustical dual source measurements, *J. Acoust. Soc. Am.*, **113** (2003) 2754-2761.
46. S. Mueller and P. Massarani, Transfer-Function Measurement with Sweeps, *J. Audio Eng. Soc.* **49** (2001) 443-471.
47. D. Bradley and L. M. Wang: The effects of simple coupled volume geometry on the objective and subjective results from nonexponential decay, *J. Acoust. Soc. Am.* **118** (2005) 1480-1490.
48. M. R. Schroeder, New method of measuring reverberation time, *J. Acoust. Soc. Am.* **37** (1965) 409-412.
49. N. Xiang, Evaluation of reverberation times using a non-linear regression approach, *J. Acoust. Soc. Am.* **98** (1995) 2112-2121.
50. L. Faiget, C. Legros, and R. Ruiz, Optimization of the impulse response length: Application to Noisy and highly reverberant rooms, *J. Audio Eng. Soc.* **46** (1998) 741-750.
51. N. Xiang, and P. M. Goggans, Evaluation of decay times in coupled spaces: Bayesian parameter estimation, *J. Acoust. Soc. Am.* **110** (2001) 1415-1424.
52. N. Xiang, and T. Jasa, Evaluation of decay times in coupled spaces: An efficient search algorithm within the Bayesian framework, *J. Acoust. Soc. Am.*, **120** (2006) 3744-3749.
53. N. Xiang, P. M. Goggans, Evaluation of decay times in coupled spaces: Bayesian decay model selection, *J. Acoust. Soc. Am.* **113** (2003) 2685-2697.
54. N. Xiang, P. M. Goggans, T. Jasa, and M. Kleiner, Evaluation of decay times in coupled spaces: Reliability analysis of Bayesian decay time estimation, *J. Acoust. Soc. Am.*, **117** (2005) 3707-3715.
55. ISO 3382, "Acoustics – Measurement of the reverberation time of rooms with reference to other parameters," (1997).
56. J. E. Summers, R. R. Torres, and Y. Shimizu, Estimating mid-frequency effects of aperture diffraction on reverberant-energy decay in coupled-room auditoria, *Building Acoust.* **11**, 271-291 (2004).
57. J. E. Summers: Frequency-dependent models of sound fields in coupled-room concert halls, *Proc. WESPAC IX, The 9th Western Pacific Acoustics Conference*, Seoul, 26-28 June 2006. (Electronic copies are available from the author.)
58. H. Pu, X. Qiu, and J. Wang, A study on the energy exchange in coupled volumes, *J. Sound & Vib.* (2007, submitted)